Modelling pollution dispersal around Solomon Islands and Vanuatu

Jennifer A. Graham[a], David Haverson[a], John Bacon[a]

[a]*Centre for Environment, Fisheries and Aquaculture Science, Pakefield Road, Lowestoft, NR33 0HT, UK*

Abstract

To assess potential dispersion of pollutants around Honiara, Solomon Islands, and Port Vila, Vanuatu, 3D ocean circulation models were developed using Telemac-3D. A series of scenarios then explore the vulnerability of the system and test potential control measures. Results show that high coastal concentrations are most likely during the wet season, with increased volumes of discharge as well as favourable wind speed and direction. Buoyant plumes flow along the coastline, and high concentrations build up in enclosed bays. Control measures tested focus on consolidating existing outflows at depth off-shore. This results in an overall reduction of surface concentrations along the coastline. However, the reduction is dependent on the depth, off-shore positioning, and volume of outflow. With increased concentrations then found at depth, the subsequent impact on off-shore and benthic ecosystems would also need to be considered.

Keywords: Ocean modelling, Marine pollution, Water quality, South Pacific, Small Island Developing States

1. Introduction

The South Pacific contains many small island developing states (SIDS). SIDS face unique challenges in their development associated with their island locations, with populations dispersed across small islands, with limited land resources. They are often remote from neighbouring countries, particularly in the vast Pacific Ocean. These island nations are then dependent on the surrounding ocean for many reasons, and are also sensitive to changes, e.g. in sea level rise, fish stocks, or water quality (CMEP, 2018). Water quality issues have become increasingly more important as population, tourism and coastal infrastructure grow and expand (Morrison, 1999).

The Commonwealth Marine Economies Programme (CMEP) is working with SIDS across the South Pacific, to assess the current environmental status of their oceans, and advise on how they can manage sustainable development through the future (McManus et al., 2019). In this study, we particularly consider pollution dispersal, with its potential impacts on water quality around the Solomon Islands and Vanuatu. These two nations are formed of archipelagos in the southwest Pacific. However, the focus here is on their main centres of population. For Solomon Islands, the capital of Honiara is found on Guadalcanal; for

Vanuatu, the capital Port Vila is found on Efate. As populations grow rapidly within limited coastal areas, this can place significant stress on local infrastructure, and hence the surrounding environment.

With limited observations to date in these coastal regions, a major aim of the CMEP has been to gather data. However, with observations still sparse in both space and time, hydrodynamical modelling can be a vital tool for understanding conditions throughout the region. As part of the CMEP water quality assessment, the aim of this hydrodynamic modelling project has been to assess the likely extent of pollutant dispersion, from Honiara and Port Vila, and test potential control mechanisms. Ocean models can be used to assess dispersion from different locations, and under different oceanographic conditions. The models developed here have sufficient resolution to provide detail along the local coastline (with grid spacing $\leq 100\,\mathrm{m}$) and therefore represent circulation around these two locations, but also cover a wide enough extent to include impact of larger-scale ocean currents. The results here demonstrate the capability of model simulations to show how concentrated pollutants released directly through coastal outfall pipes, or into rivers that outflow to the ocean, can disperse or accumulate depending upon physical conditions.

2. Geography and physical setting

The Solomon Islands consist of an archipelago of 6 major, and over 900 smaller islands, formed of both volcanic islands and coral atolls. The archipelago is found along the western edge of the Pacific Ocean, extending between $\sim 6-11^{o}$S. The administrative capital, Honiara, is situated on the northern coast of one of the larger islands, Guadalcanal (Figure 1a).

The topography around the Solomon Islands is complex, separating the relatively deep ocean floors of the Equatorial Pacific and Solomon Sea, to the northeast and southwest, respectively. To the southwest of the islands, deep ocean trenches are found along the boundary of the Pacific and Australian Plates (depths $> 5000\,\mathrm{m}$; Figure 1). The islands themselves are also separated by deep channels and canyons, with lateral shelf gradients between channels and the coastal zone of up to 13%.

Vanuatu, also in the South Pacific, is formed from an archipelago of over 80 islands. The chain of islands is of volcanic origin, lying over the subduction zone between the Australian and Pacific plates. The capital of Vanuatu is Port Vila, situated on the island of Efate (Figure 1b).

The Solomon Islands lie within the western Pacific warm pool (e.g. Ganachaud et al., 2014), and therefore have an ocean-equatorial climate, with average temperatures around 27°C and high humidity. While there is little seasonality in temperature, there are pronounced changes in wind stress and rainfall throughout the year. June to August is a cooler, drier period, with prevailing south-easterly winds (e.g. Figure 2). Weaker north-westerly winds from November to April bring frequent rainfall and occasional cyclones. Climate variability, in terms of both wind stress and rainfall, will be influenced by the South Pacific Convergence Zone (SPCZ), and the El Nino Southern Oscillation (ENSO) (e.g. Ganachaud et al., 2014).
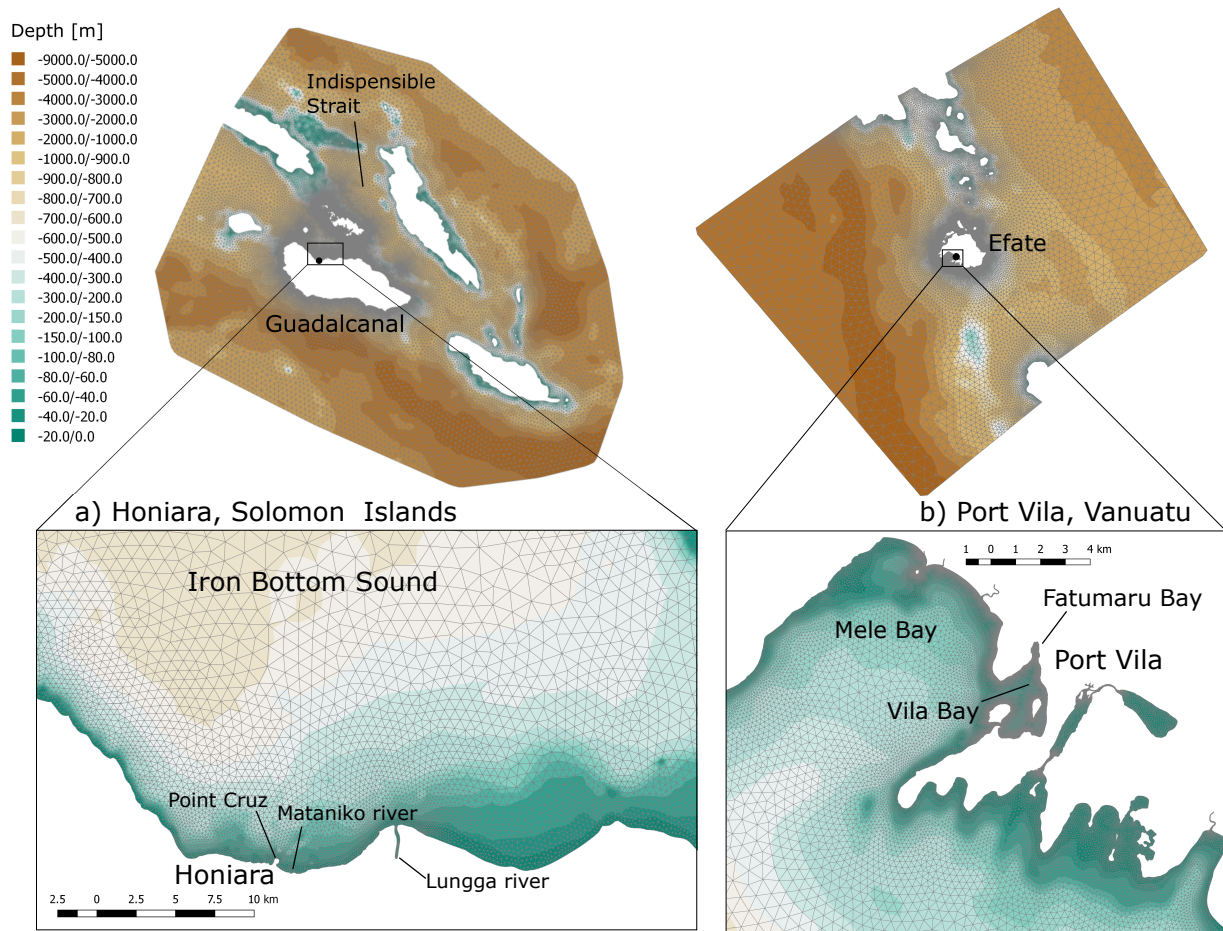
Figure 1: Bathymetry and model domain for a) Solomon Islands and b) Vanuatu. Upper panels show the extent of model domains around Guadalcanal and Efate. Lower panels show increased resolution is focussed around Honiara and Port Vila, respectively. Labels indicate locations of interest referred to in text.

Vanuatu has some similar seasonality to the Solomon Islands, but being further south, has a cooler and less humid climate overall. There is a seasonal change in wind stress, leading to alternating wet and dry seasons during the year. Weaker winds typically occur during December to March, compared with stronger south-easterlies during May-September (Figure 2). These winds are associated with the hot and wet, and cool and dry seasons, respectively. Variability in climate will be influenced by changes in ENSO and the SPCZ. However, Vanuatu also has an increased risk of tropical cyclones throughout the wet season, with the most significant of recent impacts being cyclone Pam, in March 2015. The influence of such storms can be seen as peaks in wind speed, and alternating direction, in Figure 2c-d (for example with cyclone Cook in April 2017).

Historically there have been few oceanographic observations in the southwest Pacific. However, recent
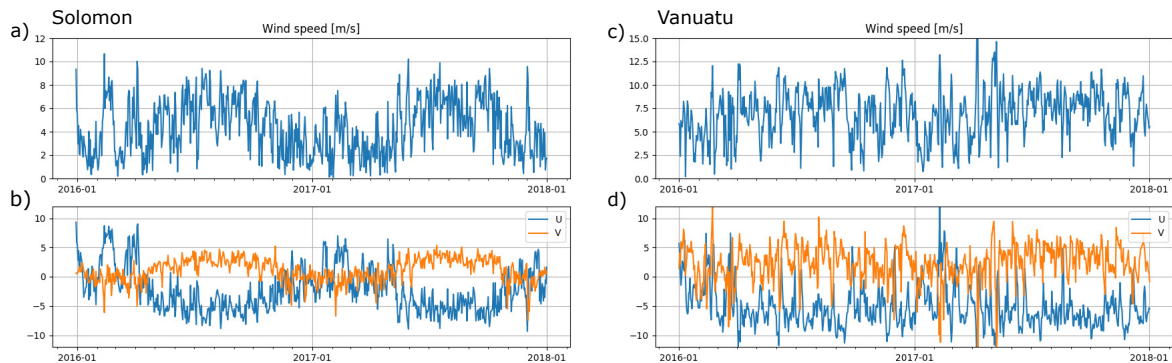
Figure 2: Daily wind speed [m/s] at a-b) Honiara, Solomon Islands; c-d) Port Vila, Vanuatu. Upper panels show wind speed; lower panels show the corresponding U and V components, where positive values are in the eastward and northward direction, respectively. Data shown was obtained from ERA5 atmospheric reanalysis (Copernicus Climate Change Service (C3S), 2017).

research campaigns, including the Southwest Pacific Ocean Circulation and Climate Experiment (Ganachaud et al., 2014), have led to a significant increase in observations. Regional modelling efforts have also increased, to represent large-scale currents as well as smaller scale features in the Solomon and Coral Seas (with grid spacing $3 - 4$ km; e.g. Djath et al. (2014); Hristova et al. (2014)). This combination of models and observations has helped to map the pathways of major currents and their variability, connecting the South Pacific and regional Solomon and Coral Seas.

The broad South Equatorial Current flows westward in the South Pacific. As this encounters island chains in the western Pacific, the current splits around the islands, forming jets. For example, the North Vanuatu Jet then flows westward between the Vanuatu and Solomon Islands. Transport also occurs on smaller scales through narrow passages within the islands (e.g. Figure 3). However, the location and strength of these is dependent on the bathymetry. For example, Iron Bottom Sound (off-shore from Honiara) is bounded by both islands and shallower bathymetry, restricting flow through the region. Stronger currents are found to the north and south of Guadalcanal, particularly through the deeper channel of Indispensable Strait (e.g. Figure 3a; Djath et al. (2014)).

Variability in wind stress also results in variability in ocean currents. Around Guadalcanal, this leads to stronger currents from the Pacific during June-September, and weaker currents during November-January (Figure 3a-b). Currents within the Vanuatu archipelago are typically weaker than those found between the Solomon Islands, with a less visible seasonal cycle (Figure 3c-d). Around Efate, a mean anticlockwise flow is seen around the island through most of the year.

While the recent research effort has significantly improved our understanding of circulation within and between the deeper ocean basins, there is still limited information for the shallow coastal seas. Model resolutions of $3 - 4$ km struggle to represent the coastlines around individual islands (e.g. Figure 1), and the
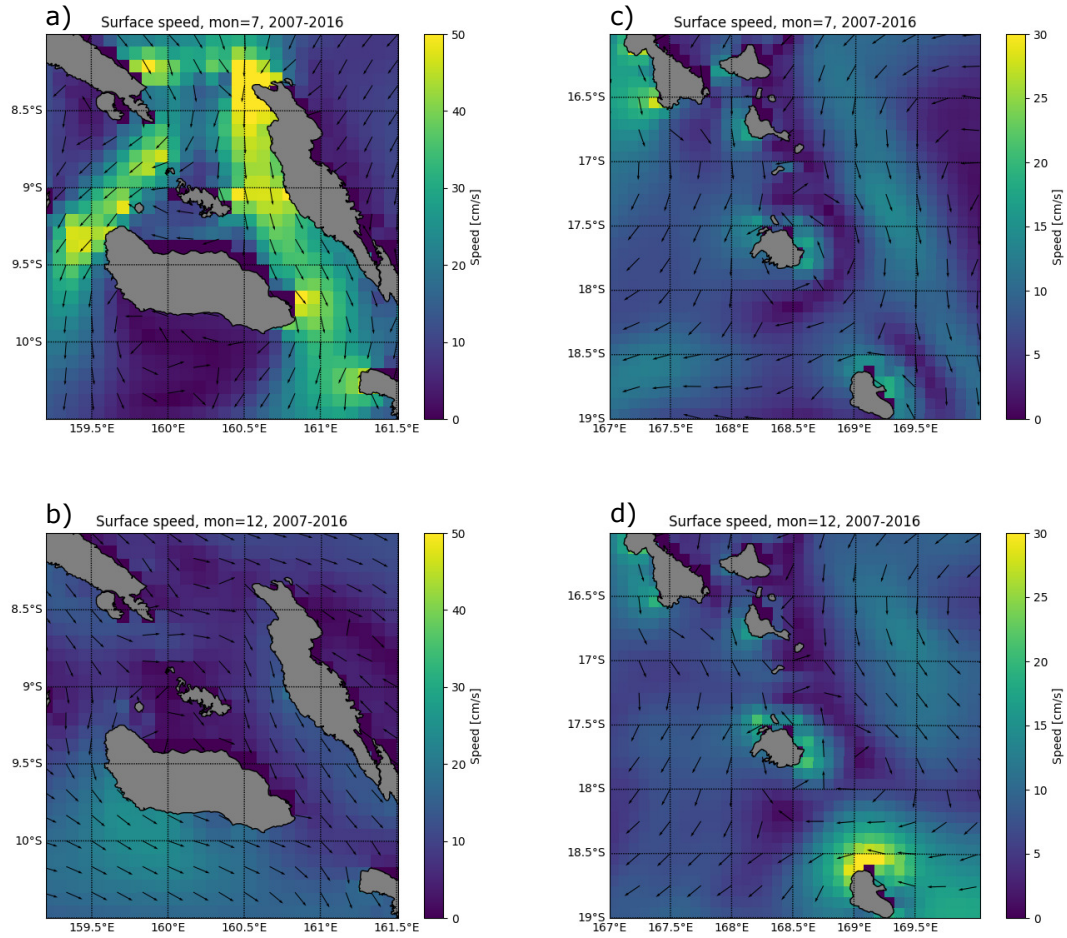
Figure 3: Mean surface currents around a-b) Guadalcanal, Solomon Islands; c-d) Efate, Vanuatu. Data shown were obtained from E.U Copernicus Marine Services Information (2019).

majority of observations available for model validation are still focussed in the deeper ocean (e.g. Ganachaud et al. (2014); Hristova and Kessler (2012); Cravatte et al. (2015)). Many global and regional models also neglect the influence of tides, which can have a significant impact on coastal currents.

3. Methods

3.1. Core model description

To investigate the spread of contaminants in the coastal ocean, regional models have been developed for both the Solomon Islands and Vanuatu. The modelling system used here is Telemac-3D (v7p2r2; Electricité de France (EDF) (2017); Hervouet (2007)). This model provides a variable grid resolution (with an unstructured triangular mesh), and varying complexity, dependent on the region and processes of interest.

To assess potential impact on surrounding populations, the focus here will be on surface concentration of contaminants rather than depth-averaged concentration. While Telemac can be used in a barotropic (2D) mode, a 3D model is then necessary, to inform on both the vertical and horizontal extent of dispersion. This also allows the model to resolve flows in both the shallow coastal zones of interest, and through deep trenches between the islands. Further details on the model grid, forcing and treatment of baroclinic processes can be found in the following sections (3.2 - 3.5).

The Telemac-3D model configuration here uses the hydrostatic approximation. Whilst this may not be realistic on the scale of individual estuaries, given the wider bays of interest here (resolutions of $< 100\,\mathrm{m}$ up to $5\,\mathrm{km}$), this is a reasonable approximation for the configuration. Use of the non-hydrostatic approximation also increases computation time significantly (runtimes increase by approximately 50%), so would limit the periods and scenarios that would be feasible to explore here.

Treatment of tidal flats is included within both configurations, such that the free surface gradient is corrected wherever dry areas are detected. Advection of velocity and tracers is then handled using the MURD (Multidimensional Upwind Residual Distribution) scheme adapted for use with tidal flats. Horizontal turbulence is modelled using the Smagorinsky scheme, which provides a turbulent viscosity dependent on the size of resolved motions and therefore on the size of the mesh spacing. The $k - \varepsilon$ model was considered as an alternative, however this proved to be less stable than Smagorinsky in these configurations, and was therefore discounted for this study. A mixing length model is used for vertical turbulence, with the Quetin option chosen to allow representation of wind drift in the surface boundary layer (Gauthier and Quetin, 1977). Bed friction in the model is applied by using the Law of Nikuradse with a roughness length equal to $0.01\,\mathrm{m}$, suitable for a rippled non-cohesive granular bed. This is applied as a constant over the model domain.

3.2. Domain and bathymetry

The study here focuses on pollutants released from the main centres of population for Solomon Islands and Vanuatu, Honiara and Port Vila, respectively. Regional models are therefore centred on these cities, with the resulting model domains shown in Figure 1. Resolution is increased along the coastlines of interest, with grid spacing $\sim 100\,\mathrm{m}$ along the coast of Honiara, and $\sim 20\,\mathrm{m}$ at the coast in Port Vila Bay. Fully resolving each individual outflow or river is not feasible for the domains considered here. However, final resolution does ensure that key features of coastline are resolved, which could influence circulation in the proximity of these outflows (e.g. Point Cruz peninsula in Honiara, and complex coastline and varying bathymetry within Vila Bay). Given this small grid spacing, a time step of $1\,\mathrm{s}$ is used for both models.

Both model domains extend into the deep ocean, off-shore, to ensure that circulation near the coast can evolve without being overly influenced by the boundary conditions. To allow for more efficient simulations (especially given the short time step), progressively coarser resolution is used away from the coast, increasing

to at least 5 km spacing at the boundary (Figure 1). Both models have 10 vertical sigma-levels, with resolution focused at the surface and base of the water column. These layers allow for more accurate representation of currents and dispersion near the sea surface, with the depth of each level, as a percentage of full depth, defined as: 1, 2, 10, 20, 50, 80, 90, 95, 98, 100 (where 1 represents the seabed, and 100 represents the sea surface). The resulting 3D meshes have 5,530 nodes and 8,802 elements for the Solomon Islands, and 6,650 nodes and 10,737 elements for Vanuatu.

Bathymetry for the Solomon Islands was obtained from two sources. Increased resolution bathymetry for the coastal zone along the north coast of Guadalcanal was acquired from Tcarta Ltd, created as a product of analysis from satellite images. Covering the key region of interest, these data comprise a synthesized dataset of 90 m resolution within Iron Bottom Sound, as well as 10 m resolution data along the northern coast of Guadalcanal. For the remainder of the domain, bathymetry is taken from the General Bathymetric Chart of the Oceans (GEBCO, Weatherall et al. (2015)) with a resolution of 30 arc-seconds (~ 1 km). The resulting model bathymetry is shown in Figure 1a.

The bathymetry across the majority of the Vanuatu domain is also sourced from GEBCO. However, additional data has been used in Mele Bay and Vila Bay. The bathymetry surrounding Efate, up to ~ 25 km from shore, was provided by Earth Observation and Environmental Services (EOMAP) at a resolution of 50 m. This is an optically clear satellite-derived bathymetry data set. Depths > 25 m in Vila Bay were provided by the UK Hydrographic Office at a resolution of 5 m. The resulting model bathymetry is shown in Figure 1b.

3.3. Boundary and Surface Forcing

For both models, tidal forcing is provided at the open ocean boundaries. Eleven tidal constituents are provided from the Topex Poseidon crossover solution (TPXO), Pacific Ocean 1/12° regional model (Egbert and Erofeeva, 2002). These TPXO harmonics are used to drive the model, with prescribed velocity and elevations along the open boundary. Tracers evolve freely through the boundary.

For the studies considered here, the major sources of pollution are at the sea surface (either in river outflows or coastal pipe discharge). Surface currents and mixing are likely to be influenced by the local wind stress. Therefore, wind forcing is applied for each model. Wind data was obtained from European Centre for Medium-Range Weather Forecasts (ECMWF) atmospheric reanalysis product, ERA5 (Copernicus Climate Change Service (C3S), 2017). The same wind forcing is applied over the domain, but varies in time, with wind speed updated at daily frequency. These daily speeds were taken from locations in Mele Bay and Iron Bottom Sound (the regions of interest for the model domain), and are shown in Figure 2.

3.4. Tracers and sources

For the study regions here, the sources of contaminants occur predominantly through freshwater outflows along the shore. Temperature and salinity are included as active tracers within the model, and determine

7

the density of the ocean. We then assume that the transport of these buoyant plumes will be dominated by salinity gradients between the outflows and surrounding seawater. While temperature gradients are found with depth (especially in the deep, open ocean), there is little difference in temperature expected in the surface mixed layer around the coast. Variability in open ocean surface salinity is also likely to be negligible compared to the difference between the open ocean and fresh sources.

For simplicity, these idealised experiments then set a constant temperature throughout the domain, but salinity differs between the ocean (initially 34.5 throughout) and each river or pipe outflow ($\sim 0\,\mathrm{PSU}$). The constant temperature and salinity in the open ocean then neglects the impact of baroclinic currents. However, the salinity gradient between the ocean and freshwater sources will result in buoyancy-driven circulation, associated with these sources (for example determining the behaviour of river plumes). Future work will investigate the impact of both temperature and salinity variability, and resulting baroclinic currents, throughout the region.

At the time of this study, there is no data available from river gauges in either the Solomon Islands or Vanuatu. However, during CMEP field campaigns in Nov-Dec 2017 and Aug 2018, flowmeter observations were obtained to estimate the flow rates of major rivers in the vicinity of Honiara and Vanuatu, respectively. While there are known to be variations in rainfall through the year (and therefore varying runoff rates), given the lack of frequent observations, river runoff is kept constant within the simulations. However, scenarios of differing pipe discharge have been used.

Outfall pipes are visible along the shoreline in both Honiara and Port Vila. While other sources may exist, there are 17 currently known around Honiara (15 along the coastline, and 2 into Mataniko river), and 17 around Port Vila Bay. The Solomon Islands Water Authority (Solomon Islands Water Authority and Hunter H20, 2017b) list a range discharges rates for Honiara, with volumes based on rainfall as well as typical use per population. The report provides three discharge rates for the existing system (in 2017):

- Average Dry Weather Flow rate (ADWF): 25.9 l/s

- Peak Dry Weather Flow rate (PDWF): 93.3 l/s

- Peak Wet Weather Flow rate (PWWF): 178.8 l/s

The majority of the simulations here will consider the largest value (PWWF), as a "worst-case" scenario. However, it is worth noting that these peak flows are based on the population in 2017. By 2022, with an increase in population (from 105,453 to 125,245) and increased proportion connected to sewage system (from 55% to 62%; Solomon Islands Water Authority and Hunter H20 (2017a)), the PDWF for Honiara is forecast to increase to 168.8 l/s (Solomon Islands Water Authority and Hunter H20, 2017b). There is little information on flowrate for Port Vila. Therefore, given similar population size of Honiara and Port Vila, the same discharge values are assumed for both model domains. For both locations, the total discharge

is then distributed between the known pipe locations. Whilst flow rates are likely to vary with time (and throughout the day), both models assume a constant flow rate for simplicity.

To investigate water quality, pollution in the model has been represented by a passive tracer. This passive tracer has been released from river sources, as well as known locations of outfall pipes along the shore. In addition to runoff or discharge rates, a concentration of tracer is then set for each source.

Water quality can be defined by a number of different parameters, many of which have been observed during the CMEP field campaigns (Devlin et al., 2019, 2018). Here, the concentration of passive tracer is scaled by the level of Dissolved Inorganic Nitrogen (DIN). This variable was chosen due to availability of observations in the region, to enable scaling of sources along the coastline. The caveat for any comparison with observations here is that DIN is an active tracer, varying with time due to chemical and biological processes in the ocean. The model does not represent these processes, and is therefore not a true water quality model, but is rather a tool for understanding the circulation in the region, and therefore potential spread of contaminants. To clarify that this is a passive tracer, hereafter we refer to the tracer as simply "pollutant". Due to the lack of previous studies around these islands, this is still a significant step forward in understanding their coastal environment.

Based on the lowest observed values in the open ocean, a background pollutant concentration was set to $5\,\mu$g/l for both domains. For river mouths, the concentration was then set to the observed concentration of DIN where available (from field campaigns in 2016 and 2017). These range from $\sim 200\,\mu$g/l for rivers in central Honiara and Port Vila, to $\sim 20\,\mu$g/l in more rural locations (Devlin et al., 2018). Rivers with no known observations were set equal to the background concentration. However, their freshwater runoff may still affect the local circulation and therefore dispersion of nearby sources.

While observations exist for the majority of central river sources, there are very limited observations directly from pipe outflows along the shore. Coastal observations show elevated concentrations (e.g. $>$ $800\,\mu$g/l in eastern Honiara), but are still diluted from true source concentrations. Two outfall pipes are known to discharge into the Mataniko river in central Honiara. To estimate the "raw" concentration at source, the difference in concentration of DIN between upstream and downstream of these pipe locations ($67\,\mu$g/l and $> 208\,\mu$g/l, respectively), was scaled up based on the ratio of river runoff volume compared to the volume of pipe outfalls. Ignoring any other potential sources, this suggests a pipe concentration of $> 50,000\,\mu$g/l.

This suggested concentration is likely an overestimate for individual pipes, given that other sources may exist along the river, and the concentration at the mouth may also be influenced by nearby pipes along the coast. However, the order of magnitude is justifiable given the total flux of DIN observed, and is also consistent with nutrient concentrations expected for untreated wastewater (e.g. Vazquez-Montiel et al., 1996). Based on these observations, the concentration for each pipe is then estimated as $10,000\,\mu$g/l. Given the uncertainty in river runoff volume, and the fact that chemical/biological processes are not included,

Table 1: List of experiments (and respective names) carried out, for both Solomon (Sol) and Vanuatu (Van) domains. Scenarios are defined in Subsection 3.5. Results for each scenarios are discussed in turn in Section 5. Note that duration stated for each follows a 30-day spin-up simulation.

Experiment	Scenario	Wind forcing/Duration	Pipe outflows
Sol_{NW}	1	1 Dec - 30 Dec 2016 (Northwesterly, wet season)	PWWF total, surface outflows
Sol_{SE}	2	1 Jul - 30 Jul 2017 (Southeasterly, dry season)	PWWF total, surface outflows
Sol_{20}	4	1 Dec - 30 Dec 2016 (Northwesterly, wet season)	PWWF total, consolidated outflow at 20 m
Sol_{50}	4	1 Dec - 30 Dec 2016 (Northwesterly, wet season)	PWWF total, consolidated outflow at 50 m
Van_{wet}	1	1 Dec - 30 Dec 2016 (Southeasterly, wet season)	PWWF total, surface outflows
Van_{dry}	3	1 Dec - 30 Dec 2016 (Southeasterly, wet season)	ADWF total, surface outflows
Van_{wet20}	4	1 Dec - 30 Dec 2016 (Southeasterly, wet season)	PWWF total, consolidated outflow at 20 m
Van_{dry20}	4	1 Dec - 30 Dec 2016 (Southeasterly, wet season)	ADWF total, consolidated outflow at 20 m

this is a reasonable assumption to apply for the simulations. This magnitude is also further supported by observations from one pipe in Vanuatu, where a concentration of $4,451\,\mu\text{g/l}$ was observed in 2016.

As with the flow rate, the source concentration of each tracer is held constant with time in the model. Tracer diffusion coefficients were set to $0.1\,\text{m}^2/\text{s}$ in the horizontal, and $0.1\,\text{m}^2/\text{s}$ in the vertical.

3.5. Experimental design

Model simulations here are used to give an indication of how pollutants are likely to spread under different scenarios. A 30 day spin-up simulation precedes each scenario, to establish the coastal circulation with no pollutant release. For each scenario, the model is then run for 30 days, with the initial pollutant concentration set to background levels and evolving thereafter. The 30-day duration allows for residual circulation and dispersal to be determined over the course of a spring-neap cycle. A full list of experiments for Solomon Islands (Sol) and Vanuatu (Van) is outlined in Table 1, with scenarios outlined as follows:

- Scenario 1: Control simulations under December wind conditions (Sol_{NW} and Van_{wet}).

- Scenario 2: Impact of seasonality in wind forcing for Solomon (Sol_{SE}).

- Scenario 3: Impact of runoff rates in Vanuatu (Van_{dry}).

- Scenario 4: Impact of consolidating outflow at depth off-shore, compared to existing surface coastal outflows (Sol_{20}, Sol_{50}, Van_{wet20} and Van_{dry20}).

These experiments provide guidance for when concentrations are likely to be higher or lower in the region. For the Solomon Islands, Scenario 2 considers varying wind forcing between prevailing north-westerlies or south-easterlies, typical during the wet or dry seasons, respectively. Figure 2 shows that there is seasonal variability in both the speed and direction of wind forcing at Honiara. Scenario 2 then provides insight into how sensitive the dispersal of pollutants may be to changing wind stress for this location.

For Vanuatu, while there is some seasonality in wind speed (and variability associated with storms), the mean direction remains predominantly southeasterly throughout the year. The scenarios tested here then use the same period of forcing for each experiment (December, during the wet season). However, Scenario 3 investigates the impact of varying the outflow rates within pipes, comparing ADWF with PWWF conditions.

Scenario 4 is used to test potential mitigation methods for both Honiara and Port Vila. Whilst there is no real substitute for sewage treatment before disposal, this investigates potential future development of the pipeline system (e.g. as suggested in Solomon Islands Water Authority and Hunter H20 (2017a)).

It is worth emphasising again that these are idealised scenarios. The lack of chemical and biological processes in the model means that these results should not be considered as indications of actual DIN concentrations in the surrounding ocean. Rather than focusing on potential threshold values for "safe" conditions, the focus here is instead on variability between different scenarios, and hence how local concentrations are likely to vary.

4. Validation of tidal circulation

While current observations exist for the wider vicinity of these islands (e.g. Section 2; Hristova and Kessler (2012), Cravatte et al. (2015)), there are limited observations within the coastal regions of Iron Bottom Sound and Mele Bay. However, tide gauges are available at Honiara (Point Cruz) and Port Vila (south-western Vila Bay). As the circulation in these regional models is driven initially by tidal forces, these can then be used to assess the tidal circulation. Figure 4 then shows comparison between the observed and modelled free surface. To remove the impact of any difference between the model bathymetry and depth at observed location (or drift in observations), both timeseries show the variability of free surface around the 30-day mean.

At both locations, the mean bias (model-observation) is negligible, with Figures 4a,c showing that both models reproduce the local tidal cycle. There are still anomalies visible throughout this cycle, with a root mean square error of 6.0 cm at Honiara, and 5.1 cm at Port Vila (Figures 4b,d). Some difference can be
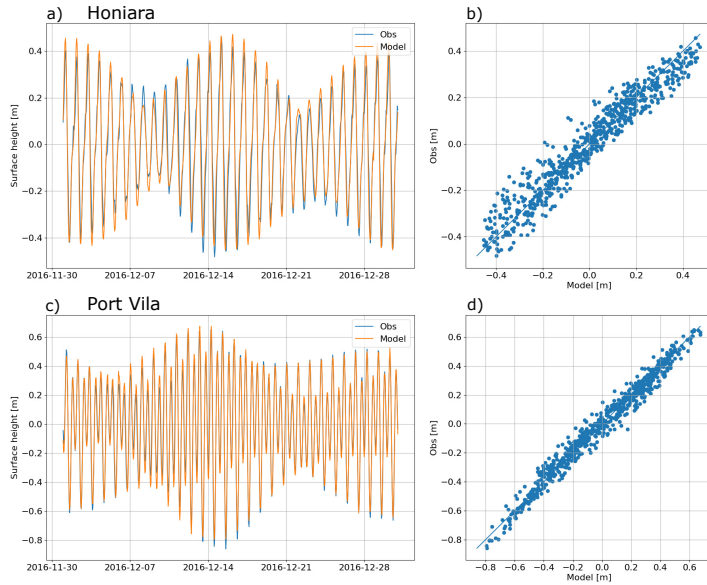
Figure 4: Variability in surface height about mean from both models and tide gauge observations [m] over December 2016, for a-b) Honiara, Solomon Islands; c-d) Port Vila, Vanuatu. Model output is taken from experiments Sol_{NW} and Van_{wet}. Tide gauge data is obtained from Pacific Sea Level Monitoring Project (2019).

expected. While these models have relatively high resolutions along the coastline, they are still unlikely to represent small-scale coastal features, such as variability in depth and port infrastructure, where these tide gauges are situated. However, this demonstrates that while there is some difference between model and observations, both models should perform well in reproducing the tidal circulation and therefore mixing at these locations.

5. Results

5.1. Scenario 1: Control

Control simulations for both Honiara and Port Vila demonstrate the impact of PWWF outflows during wind conditions that would be typical for the wet season (December; Sol_{NW} and Van_{wet}, Table 1). Results show that the highest concentrations are found near the point of source, as expected (Figures 5a and 6a). However, Port Vila and Honiara differ in the geometry of their coastlines and regional bathymetry. Honiara has a narrow coastal shelf, with depth then dropping steeply away from the coast. Vila Bay contains portions of both shallow and deeper water within the sheltered bay, but remaining $< 50\,\text{m}$ deep. This means that while the surface concentration drops off relatively quickly away from the shore around Honiara (in depths $> 20\,\text{m}$), elevated surface concentrations are found throughout Vila Bay. Particularly high concentrations are found at both the northern and southern ends of the Bay, where flow is further restricted by shallow
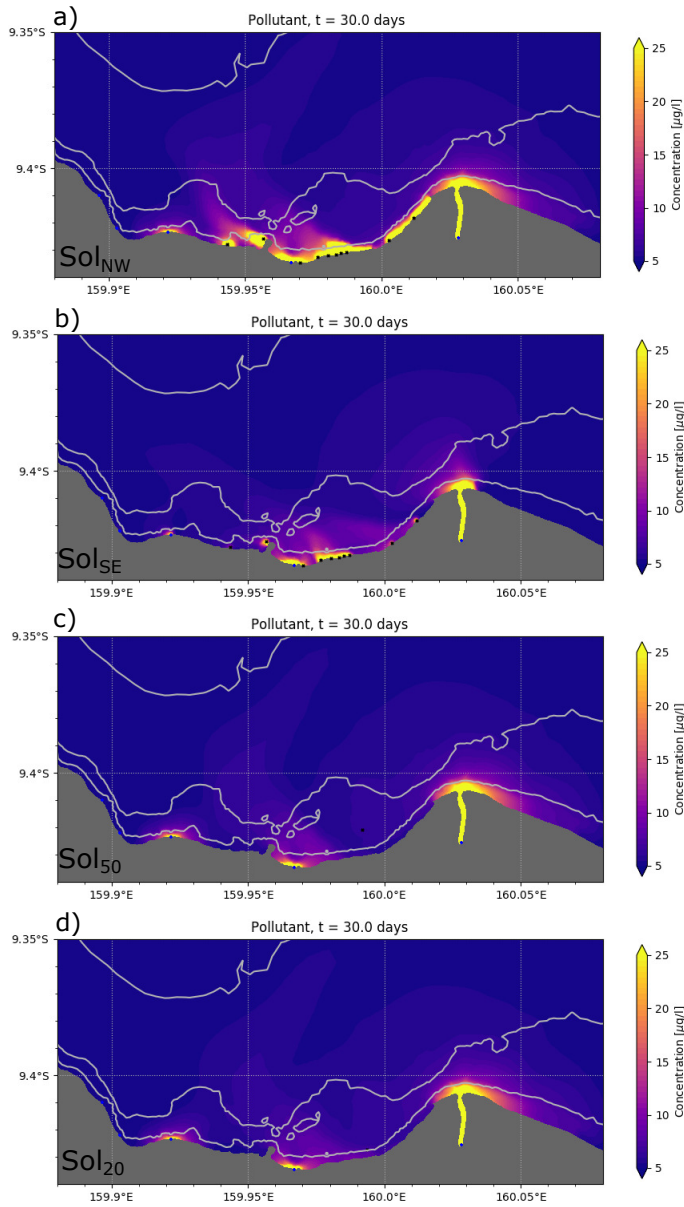
Figure 5: Surface pollutant concentration [μg/l] following 30 days of release, for various scenarios: a) Sol_{NW}; b) Sol_{SE}; c) Sol_{50}; d) Sol_{20}. Experiments are listed in Table 1. Black markers show location of sewage pipe outflows. Blue markers show location of river runoff. Grey lines show the 20, 100, and 500 m isobaths.
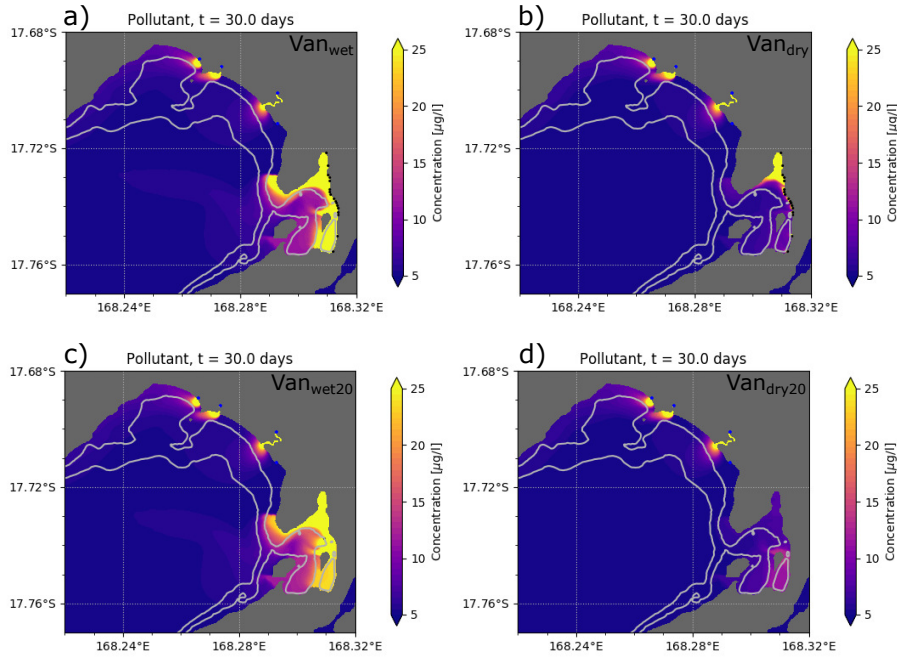
Figure 6: Surface pollutant concentration [μg/l] following 30 days of release, for various scenarios: a) Van$_{wet}$; b) Van$_{dry}$; c) Van$_{wet20}$; d) Van$_{dry20}$. Experiments are listed in Table 1. Black markers show location of sewage pipe outflows. Blue markers show location of river runoff. Grey lines show the 20 and 100 m isobaths. Line in panel d shows the location of cross sections shown in later Figure 14.

sills.

Coastline and bathymetry plays a key role in determining patterns of circulation and therefore concentrations along the coastline. Figures 7a and 8 show the residual currents over 30 days for the two regions (over a spring-neap cycle). There is a residual anti-clockwise circulation around Iron Bottom Sound. However, along the shallow coastal shelf, there is a residual westward flow.

Within Mele Bay, the combination of wind and tidal forcing leads to a residual circulation anti-clockwise around the bay. A similar pattern is seen in Vila Bay. This residual direction contributes to the increased concentrations in Fatumaru Bay, as outflows along the shore flow northwards towards the Bay (in addition to the five pipes discharging directly into Fatumaru Bay). There is also a net outflow from Vila Bay at the surface (due to the freshwater pipe outflows), and currents are stronger along the northern coast of Vila Bay. Increased concentrations are then found on the southeastern side of Mele Bay, due to the influence of these outflows.

In general, for both regions, increased currents are found in the vicinity of river outflows, and over shallow bathymetry. This is more evident around Honiara, where there is a larger volume of river runoff, particularly in the Lungga River. Although the source concentration in the Lungga (40 μg/l) is less than that within

14

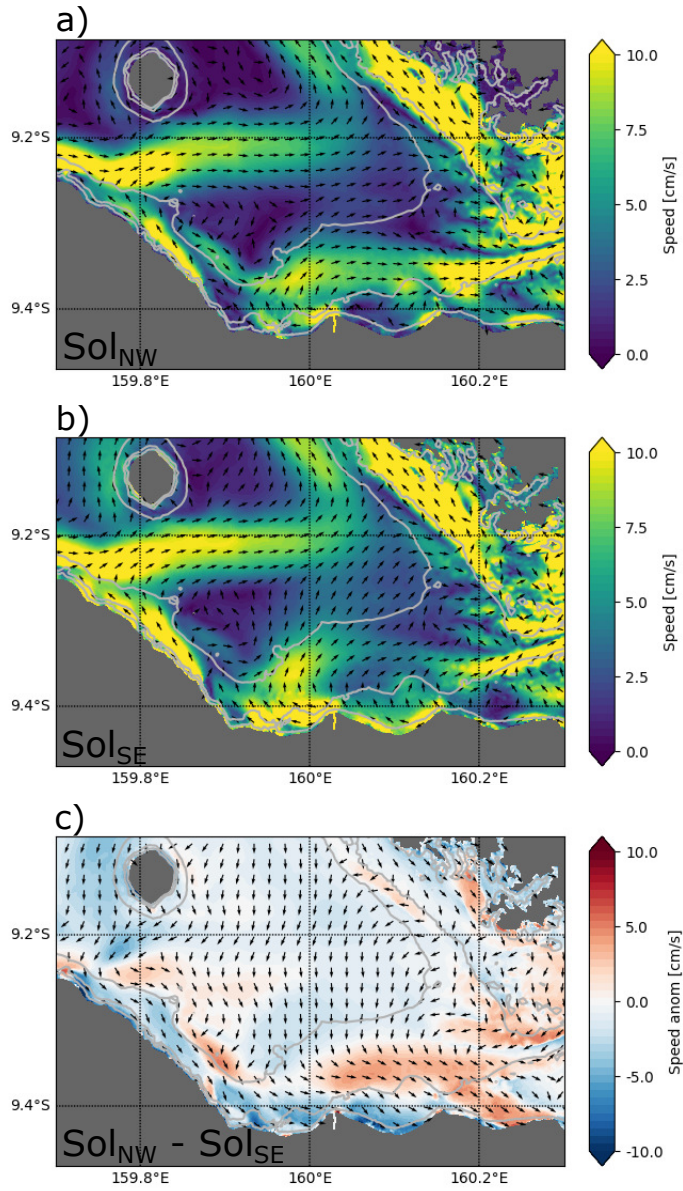Figure 7: Residual surface currents (30-day mean) for region surrounding Honiara, under a) December, north-westerly wind conditions (Sol_{NW}); b) July, south-easterly wind conditions (Sol_{SE}). Panel c) shows the anomaly for Sol_{NW} - Sol_{SE}. In each panel, shading indicates the magnitude of wind speed [cm s^{-1}], arrows show the mean direction of absolute wind speed and anomalies. Grey lines show the 20, 100, and 500 m isobaths.
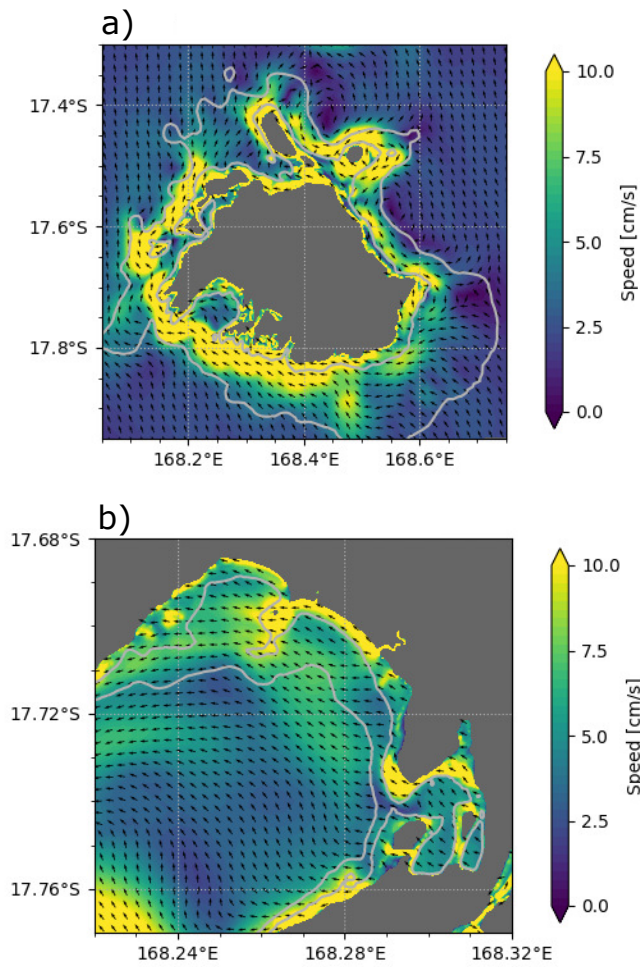
Figure 8: Residual surface currents (30-day mean) for regions surrounding a) Efate; b) Port Vila and Mele Bay. Both figures show results from the same simulation, with December, south-easterly wind conditions (Van_{wet}). In each panel, shading indicates the magnitude of wind speed [cm s^{-1}], arrows show the mean direction of absolute wind speed and anomalies. Grey lines show the a) 100, and 500 m isobaths; b) 20, and 100 m isobaths.

the outfall pipes ($10,000\,\mu$g/l), or in the Mataniko River ($210\,\mu$g/l), the volume of discharge ($\sim 42.0\,\mathrm{m}^3$/s and $3.8\,\mathrm{m}^3$/s, for the Lungga and Mataniko rivers, respectively) means that there is a wider impact on the coastline due to the plume extent. In the southern hemisphere, coriolis forces will encourage buoyant freshwater plumes to flow with the coast to their left. However, the influence of residual tidal circulation, and the prevailing wind direction, does cause variations along the coastline (and will be discussed further in Subsection 5.2).

In central Honiara, Point Cruz peninsula is found to the west of the Mataniko river mouth. This restricts flow from the Mataniko flowing further west along the coast. Along with a lower number of outfall pipes along the western coastline, this contributes to overall lower concentrations in the west, compared with the east. However, an outflow pipe on the western side of Point Cruz does still cause the high concentrations visible here (Figure 5a).

5.2. Scenario 2: Impact of wind stress

Both locations show variability in wind speed during the year (Figure 2). For Honiara, there is a marked change in both wind speed and direction between the seasons. Therefore, Scenario 2 investigates the impact of this seasonality (Sol_{NW} and Sol_{SE}, Table 1). While the change in wind stress is typically also accompanied by rainfall, both these experiments consider PWWF, but with wind forcing from either December (Sol_{NW}) or July (Sol_{SE}).

Figure 7 shows that this change in wind stress has an impact on the surface ocean currents. While the large-scale residual currents appear similar (Figure 7a-b), the anomalies show that weaker, northwesterly winds during the wet season can lead to reduced off-shore flow from the coast (Figure 7c). Surface concentrations of pollutant also show similar large-scale patterns, with the largest concentrations at the point of source along the coast, compared with dispersion off-shore (Figure 5a-b). However, the anomalies between these simulations show that there is a higher surface concentration at the coast during Sol_{NW} (Figure 9a).

This shows that aside from any change in runoff volume during the wet season, the wind conditions will be favourable for increased surface concentrations. This result can initially be attributed to the change in surface currents, reducing off-shore dispersion (Figure 7c). However, along with the change in wind direction, there is also an increased wind speed during July (Sol_{SE}, Figure 2). Increased wind stress will increase mixing in the surface layer, distributing pollutant through greater depth, and therefore reducing surface concentrations. It is likely that the results for this Scenario are down to a combination of these forcing mechanisms.

Port Vila sees some similar seasonality, with a mean reduction in wind speed during the wet season. Although this has not been tested here, it is therefore likely that such conditions would also be favourable for higher surface concentrations. However, the peak wind speeds associated with tropical storms are likely to increase mixing in the region. Such processes would have to be considered along with the increased rainfall
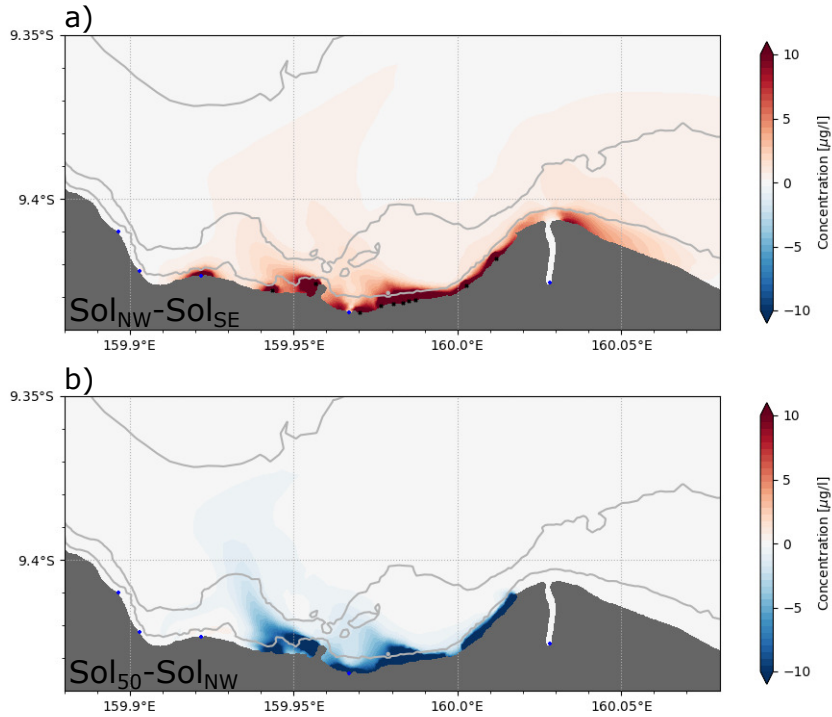
Figure 9: Surface pollutant concentration anomalies [μg/l] for a) Sol_{NW}-Sol_{SE}; b) Sol_{50}-Sol_{NW}. Panel a shows anomalies averaged over 30 days of release (to account for differing tidal cycles between the two simulations);b shows the anomaly following 30 days of release (on the same day). Black markers show location of coastal sewage pipe outflows for NW scenario. Blue markers show location of river runoff. Grey lines show the 20, 100, and 500 m isobaths.

associated with the storm, and therefore increased runoff in the region, to decide on the likely dominant impacts.

5.3. Scenario 3: Impact of runoff rates

Both Honiara and Port Vila experience large variability in rainfall during the year. Increased rainfall will lead to larger volumes of runoff through drainage systems as well as rivers. With the absence of river gauge data, the focus here is on varying outfall pipes, considering a typical average dry weather flow (ADWF) compared to peak wet weather flow (PWWF) discharges. With limited information on how concentration may vary during the year, the concentration of each outfall is kept the same in this scenario. Therefore, the volume of pollutant released will vary directly with changes in outflow volume. While Scenario 2 considered the impact of wind stress in Honiara, Scenario 3 focuses on Port Vila, comparing Van_{dry} and Van_{wet}, respectively.

As expected, reducing the discharge volume leads to lower concentrations throughout Vila Bay (Figures 6a-b and 10a). As the river runoff is kept constant, there is little impact along the shore of Mele Bay.

However, there is a visible reduction in concentration associated with flow exiting Vila Bay.

While there is a significant reduction in surface concentration overall, there are still regions of elevated concentrations. In addition to high concentrations in the immediate vicinity of outflows, Fatumaru Bay still has widespread concentrations exceeding $25\,\mu$g/L. The shallow sill at the entrance to this bay still leads to an accumulation of pollutant. Similarly, the southeastern corner of Vila Bay is partially enclosed by surrounding bathymetry. Here, although there are fewer pipes discharging into the area, concentrations also increase due to restricted flow through the region.

These results demonstrate that while concentrations are likely to be lower during dry weather, there are regions within the Bay that are likely to be at risk from higher concentrations throughout the year. Restricted flow into and out of enclosed bays may also mean that elevated concentrations are retained for longer periods in these regions following sporadic wet weather (e.g. during tropical storms), or other discharge events. However, to consider concentration evolution or longer residence timescales, decay rates of contaminants as well as local chemical or biological processes, would also need to be considered.

5.4. Scenario 4: Impact of moving pipes to depth off-shore

A major cause of high surface concentrations along the shoreline is release of pollutant from pipes at the sea surface along the coast. Given that these are typical freshwater sources, they will be more buoyant than the surrounding seawater. The highest concentrations then remain at the surface, with stratification limiting the strength of vertical mixing. With this in mind, Scenario 4 considers a proposed method of reducing impact of sewage along the coast, by consolidated release through pipes at greater depth, off-shore. This should lead to greater mixing (dilution) with the surrounding seawater, as the buoyant plume tends to rise, thereby reducing concentrations that reach the surface.

The experiments carried out for Honiara and Port Vila all consider consolidated outflows, and they also consider either varying depth and location (Sol_{20} and Sol_{50}), or varying outfall rates (Van_{dry20} and Van_{wet20}). For all these experiments, there is a reduction in surface concentration along the coastline (Figures 5c-d, 6c-d). However, the impact is more apparent for Honiara than Port Vila, with a consistent reduction across the region seen in Figure 9b, as opposed to the more spatially-variable response seen in Figure 10c-d.

For Honiara, Figure 5c-d shows the surface concentration of pollutant following release at either 50 or 20 m depth, respectively. Proposed plans for Honiara waste water have suggested consolidated release at a depth between $20 - 50$ m (Solomon Islands Water Authority and Hunter H20, 2017a). Both simulations show that, as expected, there is a large reduction in surface concentration. This is shown further in Figure 9b, which shows a large reduction along the coast, in the vicinity of current surface outfalls. Although not shown, the difference between surface concentrations for Sol_{50} and Sol_{20} is relatively small. However, looking at the difference sub-surface, it is clear that release at 20 m could have a larger impact on coastal waters (Figures 11 and 12).
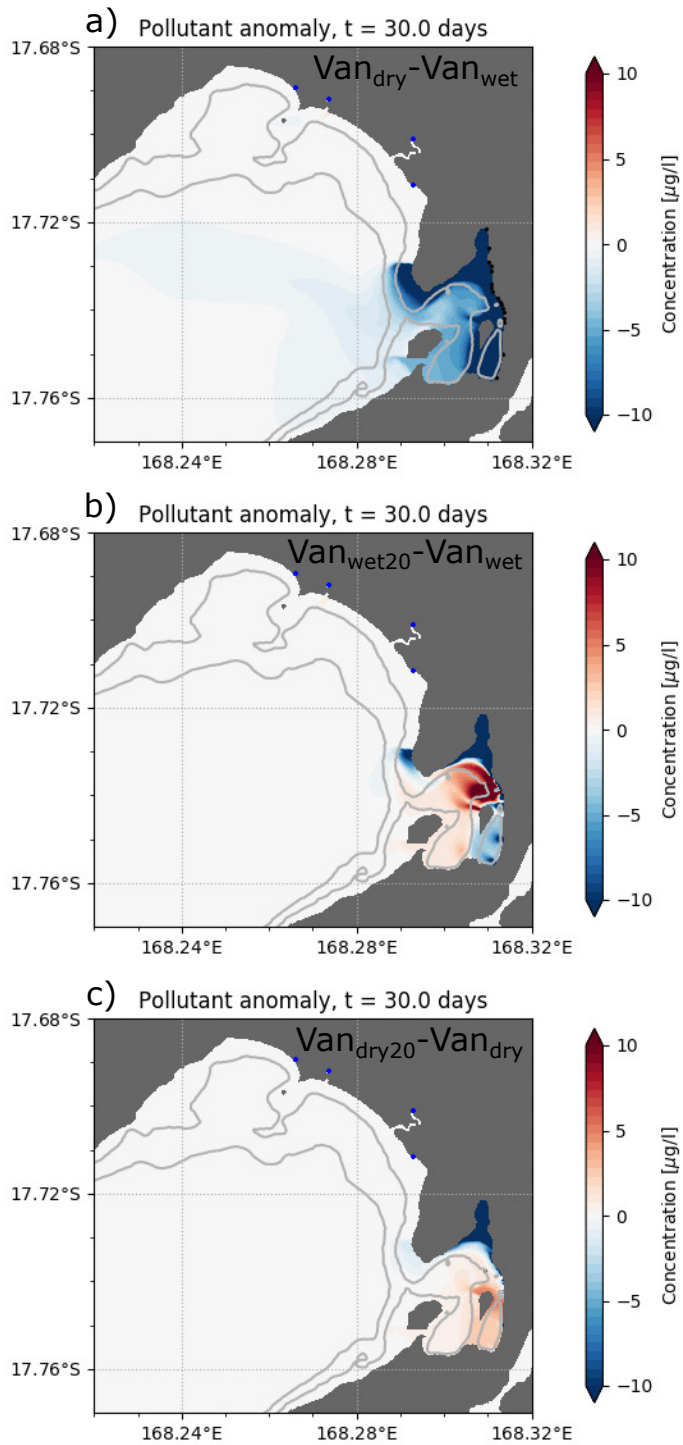
Figure 10: Surface pollutant concentration anomalies following 30 days of release [μg/l] for a) Van$_{dry}$-Van$_{wet}$; b) Van$_{wet20}$-Van$_{wet}$; c) Van$_{dry20}$-Van$_{dry}$. Black markers show location of coastal sewage pipe outflows (same locations for Van$_{wet}$ and Van$_{dry}$). Blue markers show location of river runoff. Grey lines show the 20 and 100 m isobaths.
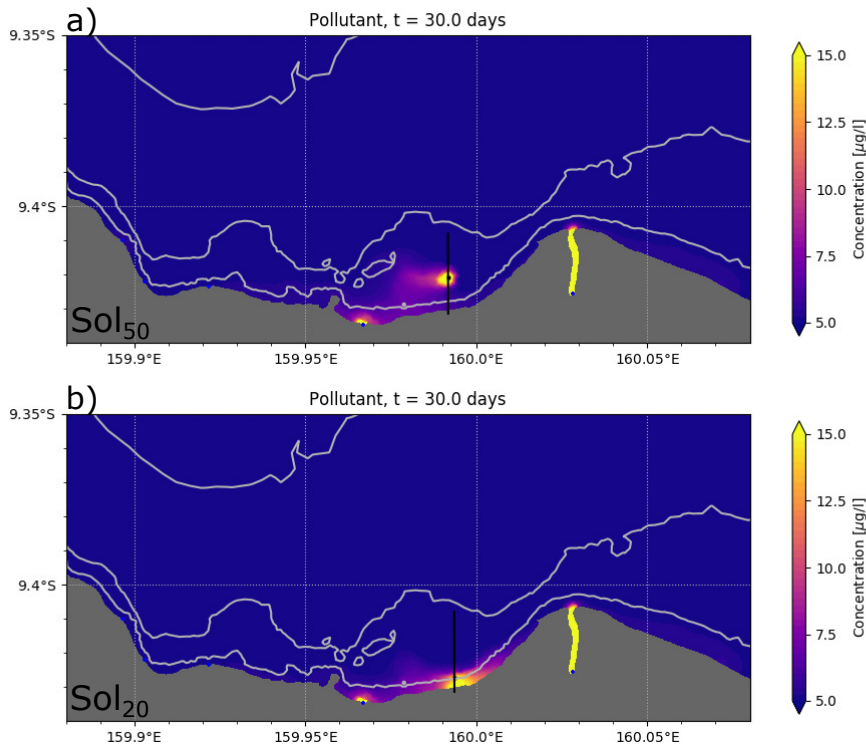
20

Figure 11: Bottom pollutant concentration [μg/l], following 30 days of consolidated release at depth, for a) Sol$_{50}$; b) Sol$_{20}$. Black markers show location of consolidated sewage pipe outflows for each scenario. Blue markers show location of river runoff. Grey lines show the 20, 100, and 500 m isobaths. Black lines show the locations of cross sections presented in Figure 12.

Ocean currents have a tendency to follow contours of equal depth (e.g. Figure 7). This means that the release at 50 m remains further from the shore as it disperses in the ocean (Figure 11a). However, the narrow shelf allows the plume from 20 m depth to bring pollutant close to shore (Figure 11b). As bathymetry drops steeply from the shore of Honiara, the 20 m depth release is only ~ 300 m from the shore, compared to ~ 1 km for release at 50 m. For a shorter, shallower pipeline, release is then closer to the coast, and closer to the surface.

In contrast to Honiara, results for Port Vila show spatial variability in anomalies within the bay (Figure 10b-c). Bathymetry is shallower than 50 m throughout Vila Bay. Therefore, only one location of release is considered here, at the 20 m isobath, close to existing pipeline systems at the northern end of the Bay (Figure 13). However, as with the surface release, experiments consider the impact of either PWWF (Van$_{wet20}$) or ADWF (Van$_{dry20}$). Both Van$_{wet20}$ and Van$_{dry20}$ show reduced concentrations in the vicinity of existing pipe locations. Both also show a large reduction within Fatumaru Bay. However, there is a differing response in central and southern Vila Bay (Figure 10).

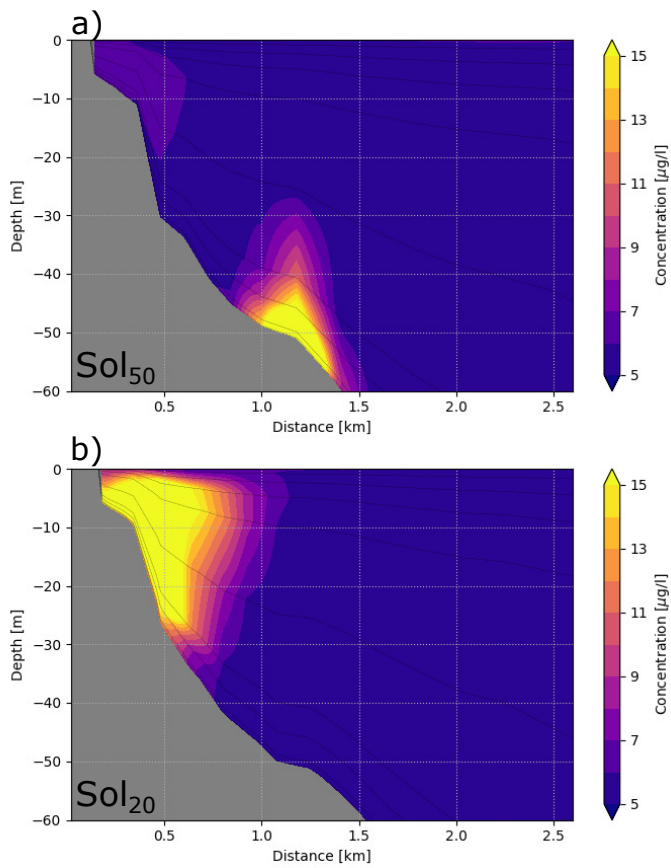As the location of release has not changed, this shows how the volume of outflow plume may affect its

21

Figure 12: Cross section of pollutant concentration [μg/l], following 30 days of release, for a) Sol_{50} (50 m depth outflow); b) Sol_{20} (20 m depth outflow). Locations of each cross section relative to outfalls around Honiara are shown in Figure 11. Grey dashed lines indicate the depth levels of terrain-following coordinates used within the model.
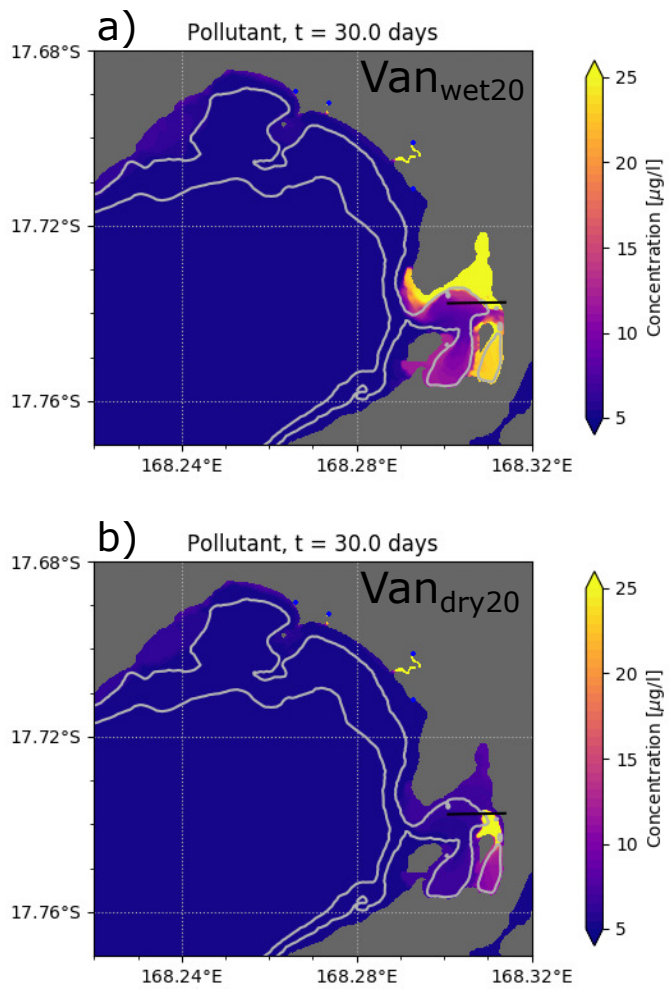
Figure 13: Bottom pollutant concentration [μg/l], following 30 days of consolidated release at depth, for a) Van$_{wet20}$; b) Van$_{dry20}$. Black markers show location of consolidated sewage pipe outflows for each scenario. Blue markers show location of river runoff. Grey lines show the 20 and 100 m isobaths. Black lines show the locations of cross sections presented in Figure 14.
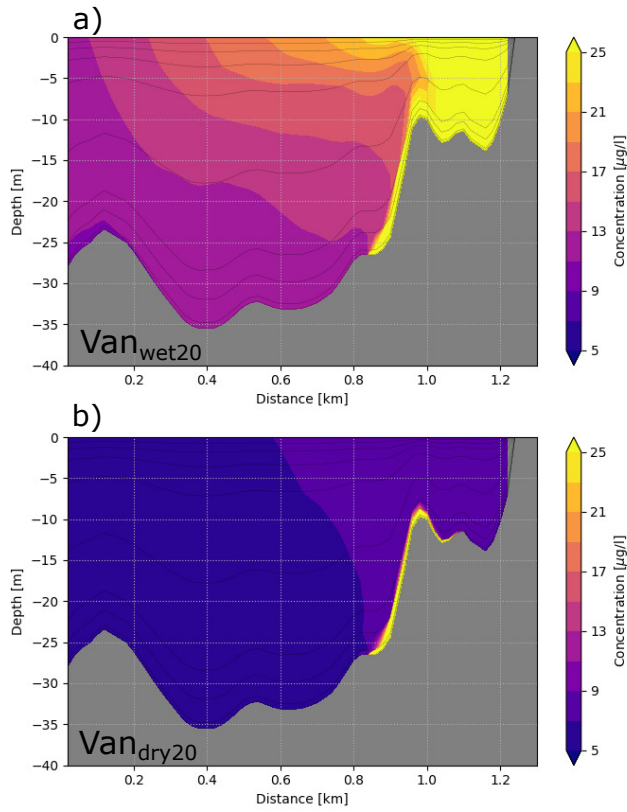
Figure 14: Cross section of pollutant concentration [μg/l], following 30 days of release at 20 m depth, for a) Van$_{wet20}$; b) Van$_{dry20}$. Locations of the cross section in Vila Bay is shown in Figure 13. Grey dashed lines indicate the depth levels of terrain-following coordinates used within the model.

trajectory of dispersion through the region. With a larger outflow, the increased buoyancy allows the plume to penetrate closer to the surface, and then also further horizontally throughout the bay (Figure 14a and 13a). With a reduced outflow, the plume remains predominantly at depth in the water column, and has a limited horizontal extent (Figure 14b and 13b). As the Van$_{wet20}$ plume reaches the surface off-shore, it contributes to increased surface concentrations in the central bay (Figure 10), whereas Van$_{dry20}$ results in increased concentrations in southern Vila Bay, as the plume spreads towards the south.

This study shows how, for release at depth, the volume of outflow can affect the trajectory of dispersal as well as the concentration. As the rising plume mixes with surrounding seawater, vertical dispersal depends on the resulting level of neutral buoyancy in the water column. As currents often vary with depth, the horizontal spread of the plume will also be influenced by its depth of neutral buoyancy. This should be kept in mind, along with any regional bathymetry that may constrain spread at this depth. A deeper plume is likely to be more constrained than one that reaches the surface.

In the studies considered here, the water column is considered to be initially fully-mixed, with constant

density. Including further stratification within the water column could then impact both the vertical and horizontal extent of the plume, and is worth further investigation. While the use of 10 vertical levels provides sufficient resolution in the coastal ocean, the terrain-following grid becomes relatively coarse in the deeper ocean (especially at mid-depth within the water column; Figures 12 and 14). This may lead to an overestimate of dispersion through the water column. Assessing the impact of vertical resolution on these scenarios would then also be worth further consideration.

For each of these experiments, it is also worth keeping in mind that while surface concentrations are reduced, the increased concentration at depth will still have an impact on ocean ecosystems. This could then have associated impacts on human health through marine food resources. In the absence of waste water treatment before disposal, such impacts would need to be considered further before future development.

6. Discussion and Conclusions

This study assesses the potential dispersion of pollutants around Honiara, Solomon Islands, and Port Vila, Vanuatu. Using 3D ocean circulation models, scenarios were tested to investigate the vulnerability of the system and potential control measures. While the pollutant release here has been scaled by available observations of DIN, the results here are applicable to any contaminant or bacteria released through the rivers or drainage systems along the coastline. For example, this includes *E. coli* and faecal coliforms, which pose risk to public health. Results show that high coastal concentrations are most likely during the wet seasons, due to increased volumes of discharge, as well as favourable wind stress. Buoyant plumes flow along the coastline, and high concentrations build up in enclosed bays. Testing consolidated outflows at depth off-shore shows overall reduction of surface concentrations along the coastline. However, the impact is not necessarily consistent within each region, with dispersal dependent on the depth, off-shore positioning, and volume of outflow.

The results here will help to inform future observations or monitoring programmes. For both regions it is likely that the current discharge system will allow any associated pollutants to remain close to shore, and in the surface ocean. To mitigate high surface concentrations, runoff could be discharged at sufficient depth and distance from the shoreline. However, it must be noted that discharge at depth will still have an impact on the ocean ecosystem, and potential food sources, with increased contaminant then at depth off-shore. There is no real substitute for fully-functioning waste-water treatment system.

The study here focuses on idealised scenarios. Future work should initially increase the complexity of the model, to demonstrate the impact of varying temperature as well as salinity, and large scale baroclinic ocean currents. With increased stratification in the ocean, the impact of non-hydrostatic processes and vertical turbulence models should also be explored, to assess the impact on vertical dispersal from buoyant outfalls. In addition to this, introducing water quality processes will inform on likely timescales for any pollutants to

decay in the region following release. Such analysis would be required to more accurately assess the off-shore extent, or recovery time following one-off events.

For Vanuatu, tropical cyclones pose a significant threat to the region. While this study has demonstrated potential influence of changes in either runoff or wind stress, the impact of extreme weather events (causing significant changes in both factors) has not been considered here. This is worth further study, to assess both the short term and potential long-term impact of extreme weather in the region.

Further observations and monitoring are also vital to establish the current baseline conditions and variability in the region. This will further inform model simulations, as well as validation of results. There are a number of caveats in this study, and prospects for future work. However, given the lack of previous studies available, this article presents an important first step in our understanding of coastal circulation and therefore transport of pollutants around these Pacific island states.

Acknowledgements

References

CMEP, 2018. Pacific Marine Climate Change Report Card 2018. (Eds. Bryony Townhill, Paul Buckley, Jeremy Hills, Tommy Moore, Sylvie Goyet, Awnesh Singh, Gilianne Brodie, Patrick Pringle, Sunny Seuseu, Tiffany Straza). Commonwealth Marine Economies Programme.

Copernicus Climate Change Service (C3S), 2017. ERA5: Fifth generation of ECMWF atmospheric reanalyses of the global climate. Copernicus Climate Change Service Climate Data Store (CDS), accessed: 2018. https://cds.climate.copernicus.eu.

Cravatte, S., Kestenare, E., Eldin, G., Ganachaud, A., Lefèvre, J., Marin, F., Menkes, C., Aucan, J., 2015. Regional circulation around new caledonia from two decades of observations. Journal of Marine Systems 148, 249–271. doi:10.1016/j.jmarsys.2015.03.004.

Devlin, M., Bacon, J., Haverson, D., Graham, J., Smith, A., Bremner, J., Petus, C., Townhill, B., Howes, E., Tracey, D., Lincoln, S., Vannoni, M., Benson, L., 2018. Pacific Water Quality and Resilience Framework - Year 2 report. Commonwealth Marine Economies Programme.

Devlin, M., Graves, C., Stevens, A., Lyons, B., Tracey, D., Petus, C., Bremner, J., 2019. Rapid Water Quality assessments utilising variable sources of data in Port Vila, Vanuatu. Marine Pollution Bulletin In preparation for this issue.

Djath, B., Verron, J., Melet, A., Gourdeau, L., Barnier, B., Molines, J.M., 2014. Multiscale dynamical analysis of a high-resolution numerical model simulation of the solomon sea circulation. J Geophys Res Oceans 119, 6286–6304. doi:10.1002/2013JC009695.

Egbert, G.D., Erofeeva, S.Y., 2002. Efficient inverse modeling of barotropic ocean tides. J. Atmos. Oceanic Technol. 19(2), 183–204. doi:10.1175/1520-0426(2002)019¡0183:EIMOBO¿2.0.CO;2.

Electricité de France (EDF), 2017. Telemac3d User Manual, Version 7.2.

EOMAP, . Earth observation and environmental services. Available online: www.eomap.com.

E.U Copernicus Marine Services Information, 2019. Global ocean physics reanalysis GLORYS12V1: GLOBAL_REANALYSIS_PHY_001_030.

Ganachaud, A., Cravatte, S., Melet, A., Schiller, A., Holbrook, N.J., Sloyan, B.M., Widlansky, M.J., Bowen, M., Verron, J., Wiles, P., Ridgway, K., Sutton, P., Sprintall, J., Steinberg, C., Brassington, G., Cai, W., Davis, R., Gasparin, F., Gourdeau, L., Hasegawa, T., Kessler, W., Maes, C., Takahashi, K., Richards, K.J., Send, U., 2014. The Southwest Pacific Ocean circulation and climate experiment (SPICE). J of Geophys Res 119, 7660–7686. doi:10.1002/2013JC009678.

Gauthier, M., Quetin, B., 1977. Modèles mathématiques de calcul des écoulements induits par le vent, in: 17e congrès de l'AIRH, Baden-Baden.

Hervouet, J.M., 2007. Hydrodynamics of free surface flows: Modelling with the finite element method. John Wiley & Sons, Ltd. doi:10.1002/9780470319628.

Hristova, H.G., Kessler, W.S., 2012. Surface Circulation in the Solomon Sea Derived from Lagrangian Drifter Observations. Journal of Physical Oceanography 42, 448–458. doi:10.1175/JPO-D-11-099.1.

Hristova, H.G., Kessler, W.S., McWilliams, J.C., Molemaker, M.J., 2014. Mesoscale variability and its seasonality in the Solomon and Coral Seas. J Geophys Res Oceans 119, 4669–4687. doi:10.1002/2013JC009741.

McManus, E., Collins, M., Yates, O., Sanders, M., Townhill, B., Mangi, S., Tyllianakis, E., 2019. Commonwealth SIDS and UK Overseas Territories Sustainable Fisheries Programmes: An overview of projects and benefits of official development assistance funding. Marine Policy doi:10.1016/j.marpol.2019.02.009. in press.

Morrison, R.J., 1999. The regional approach to management of marine pollution in the South Pacific. Ocean and Coastal Management 42, 503–521. doi:10.1016/S0964-5691(99)00031-9.

Pacific Sea Level Monitoring Project, 2019. Hourly sea level and meteorological data. URL: http://www.bom.gov.au/oceanography/projects/spslcmp/data/.

Solomon Islands Water Authority, Hunter H20, 2017a. Solomon Water 30 year strategic plan, 2017-2047.

Solomon Islands Water Authority, Hunter H20, 2017b. Solomon Water 5 year Action Plan 2017-2022.

Tcarta Ltd, . Tcarta Bathymetry. https://www.tcarta.com/satellite-derived-bathymetry.

Vazquez-Montiel, O., Horan, N.J., Mara, D.D., 1996. Management of domestic wastewater for reuse in irrigation. Water Science and Technology 33, 355 – 362. doi:10.1016/0273-1223(96)00438-6.

Weatherall, P., Marks, K.M., Jakobsson, M., Schmitt, T., Tani, S., Arndt, J.E., Rovere, M., Chayes, D., Ferrini, V., Wigley, R., 2015. A new digital bathymetric model of the world's oceans. Earth and Space Science 2, 331–345. doi:10.1002/2015EA000107.